NMR AND VIBRATIONAL SPECTROSCOPIC (IR AND RAMAN) ANALYSIS OF o-NITROBENZAMIDE

[1] S. Sumathi, [2] Rev Fr Xavier

[1] Department of Physics, SSM College of Engineering, Komarapalayam - 638 183, Tamilnadu, India.

[2]Department of Physics, St Joseph College of Arts and Science, Cuddalore-607001,Tamilnadu, India.

Abstract

In the present methodical study, FT-IR, FT-Raman and NMR spectra of o-nitrobenzamide are recorded and the fundamental vibrational frequencies are tabulated and assigned. The vibrational wavenumbers were computed using HF and DFT methods are assigned with the help of potential energy distribution method. Gaussian hybrid computational calculations are carried out using HF and DFT (B3LYP and B3PW91) methods with 6-31+G (d,p) and cc-pVDZ&aug-cc-pVDZ basis sets. Moreover, 1H and 13C NMR spectra have been analysed and 1H and 13C Nuclear Magnetic Resonance chemical shifts are calculated using the gauge independent atomic orbital (GIAO) method.

Introduction

o-nitrobenzamide is an organic compound, which consists of nitro, carbonyl and amide groups attached to the phenyl ring. It reacts with azo and diazo compounds to generate toxic gases. Flammable gases are formed by the reaction of o-nitrobenzamide with strong reducing agents. o-nitrobenzamide is very weak base (weaker than water). These derivatives are less basic and in fact react with strong bases to form salts. That is, they can react as acids. Mixing amides with dehydrating agents such as P_2O_5 or $SOCl_2$ generates the corresponding

nitrile. The combustion of these compounds generates mixed oxides of nitrogen (NOx). It is a stable compound and does not undergo polymerization. o-nitrobenzamide is easily oxidized by using Strong oxidizing agents. Exposure to air or moisture over prolonged periods destroys the nature of the amide.

The IUPAC name of o-nitrobenzamide is 2-Nitrobenzamide. The molecular formula of o-nitrobenzamide is $C_7H_6N_2O_3$ and the molecular weight is 166.13. It is a kind of beige crystalline powder and belongs to the classes of Aromatic Carboxylic Acids, Amides, Anilides and Carbonyl Compounds; Organic Building Blocks. Other synonyms of o-nitrobenzamide are 2-Nitrophenylformamide;benzamide, o-nitro-;2-Carbamoylnitrobenzene.

Preparation of 2-Nitrobenzamide

It can be prepared by the reaction 2-nitro-benzonitrile with Al_2O_3 and $MeSO_3H$. The reaction time is 15 minutes at reaction temperature of 120 °C. The yield is about 90%.

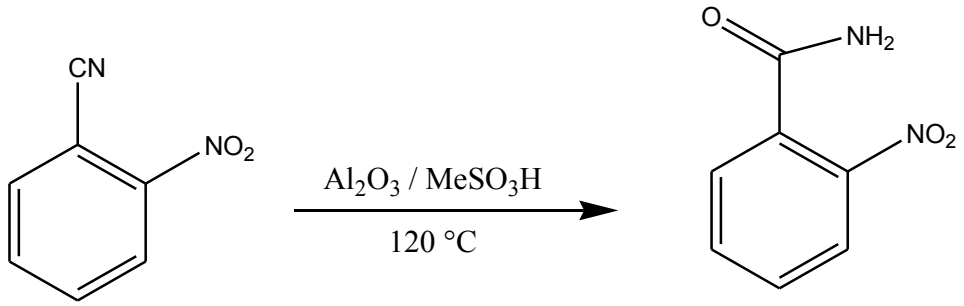

2-nitrobenzonitrile 2-nitrobenzamide

Applications

2-Nitrobenzamide was used in the synthesis of novel fluorogenicchemosensors based on urea derivative of 2-(2′-aminophenyl)-4-phenylthiazole. It was also used in the synthesis of quinazoline-2,4(1H,3H)-diones, an important class of pharmaceutical intermediates[Jiang P., et al., (2001)].

There is provided 5-(aziridin-1-yl)-4-hydroxylamino-2-nitrobenzamide for various uses, as well as pharmaceutical compositions and devices comprising 5-(aziridin-1-yl)-4-hydroxylamino-2-nitrobenzamide[Zhang H., and Cui Z., (2008)]. There are also other

methods provided for reducing reducible compounds (such as reduction-activated prodrugs, e.g. tretazicar) by contacting those compounds with α-hydroxycarbonyl compounds capable of forming cyclic dimers.

2. Experimental details

The o-nitrobenzamide is purchased from Sigma–Aldrich Chemicals, USA. The FT-IR spectrum of the compound is recorded using a Bruker IFS 66V spectrometer in the range of 4000–500 cm^{-1}. The spectral resolution is ±2 cm^{-1}. The FT-Raman spectrum of the same compound is also recorded using the same instrument with an FRA 106 Raman module equipped with an Nd:YAG laser source operating at 1.064 μm line widths with 200 mW power. The spectra are recorded in the range of 3500–400 cm^{-1} with a scanning speed of 30 cm^{-1} min^{-1} of spectral width 2 cm^{-1}. The frequencies of all sharp bands are accurate to ±1 cm^{-1}.

3. Computational methods

In the present work, HF and some of the hybrid methods, B3LYP and B3PW91, are carried out using the basis sets 6-31+G(d,p) and cc-pVDZ&aug-cc-pVDZ. All these calculations are performed using the GAUSSIAN 09W[Kuo C. H., *et al.*, 2007)] program package on an i7 processor in a personal computer. In DFT methods, B3LYP is the combination of Becke's three-parameter hybrid function, and the Lee–Yang–Parr correlation function[Carnes C.L., *et al.*, (2002),Wang H. W., *et al.*, (2002)] and B3PW91 is the combination of Becke's three parameter exact exchange-function (B3)[Yang Y., *et al.*, (2004)] and Perdew and Wang (PW91)[Deki S., *et al.*, (1998),Wang W., *et al.*, (2002)]. The optimized molecular structure of the molecule is obtained using the Gaussian 09 and Gaussview program and is shown in Fig. 1. Experimental and simulated spectra of IR and Raman are presented in Fig. 2 and 3, respectively.

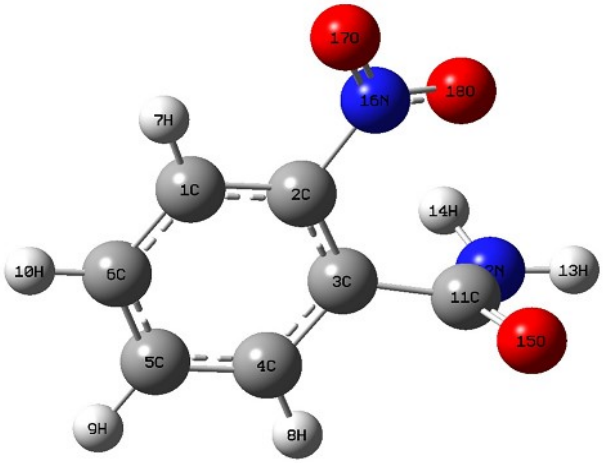

Figure 1: Molecular structure of o-Nitrobenzamide

The comparative optimized structural parameters such as bond length, bond angle and dihedral angle are presented in Table 1. The observed (FT-IR and FT-Raman) and calculated vibrational frequencies and vibrational assignments are presented in Table 2.

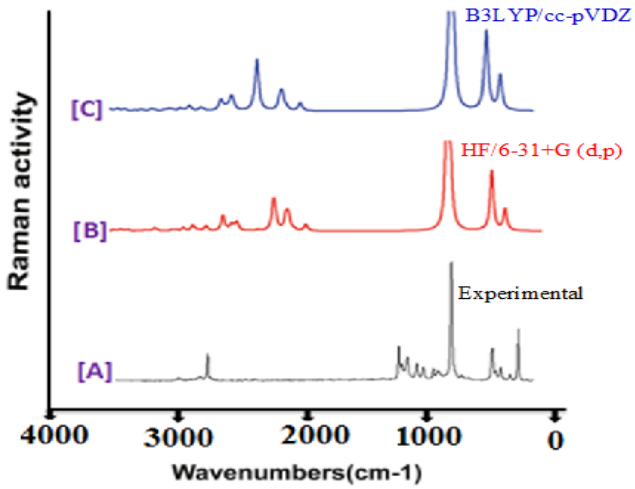

Figure 3:Experimental [A] and calculated [B&C] FT-Raman Spectra of O-Nitrobenzamide

Table 1: Optimized geometrical parameters ofo-nitrobenzamide

vs – very strong, s – strong, m – medium, w – weak, vw – very weak

Geometrical Parameter	HF/6-31+G (d, p)	B3LYP / CC-PVDZ	B3LYP/ AUG-CC-PVDZ	B3PW91/ CC-PVDZ	B3PW91/ AUG-CC-PVDZ
Bond Length (Å)					
C1-C2	1.3824	1.3965	1.3953	1.3932	1.3926
C1-C6	1.3844	1.3935	1.3947	1.3915	1.3923
C1-H7	1.0720	1.0890	1.0873	1.0896	1.0880
C2-C3	1.3885	1.4019	1.4020	1.3988	1.3989
C2-N16	1.4608	1.4787	1.4766	1.4726	1.4707
C3-C4	1.3878	1.4020	1.4012	1.3992	1.3986
C3-C11	1.5149	1.5229	1.5171	1.5181	1.5133
C4-C5	1.3873	1.3966	1.3977	1.3946	1.3953
C4-H8	1.0747	1.0915	1.0876	1.0916	1.0901
C5-C6	1.3853	1.3987	1.3980	1.3961	1.3957
C5-H9	1.0750	1.0921	1.0901	1.0921	1.0905
C6-H10	1.0743	1.0914	1.0895	1.0914	1.0899
C11-N12	1.3538	1.3695	1.3671	1.3650	1.3633
C11-O15	1.1949	1.2165	1.2201	1.2148	1.2182
N12-H13	0.9963	1.0170	1.0123	1.0157	1.0115
N12-H14	0.9939	1.0145	1.0101	1.0133	1.0094
N16-O17	1.1921	1.2234	1.2268	1.2180	1.2213
N16-O18	1.1947	1.2273	1.2287	1.2214	1.2230
Bond Angle(°)					
C2-C1-C6	119.0509	119.2607	119.1608	119.2364	119.1441
C2-C1-H7	119.5570	118.6869	119.1169	118.6622	118.9830
C6-C1-H7	121.3899	122.0522	121.7189	122.1009	121.8694
C1-C2-C3	122.3741	122.2871	122.2790	122.3120	122.3125
C1-C2-N16	117.5141	117.4046	117.5516	117.5037	117.5828
C3-C2-N16	120.0770	120.2823	120.1418	120.1508	120.0768
C2-C3-C4	117.6526	117.3564	117.5168	117.4108	117.5295
C2-C3-C11	124.1230	124.7048	124.0137	124.3306	123.9706
C4-C3-C11	117.9677	117.5738	118.1082	117.8762	118.1485
C3-C4-C5	120.8002	121.1327	120.982	121.0648	120.9504
C3-C4-H8	119.1754	118.7378	118.9565	118.7821	118.9345
C5-C4-H8	120.0145	120.1274	120.0516	120.1499	120.1057
C4-C5-C6	120.3813	120.272	120.281	120.2896	120.2985
C4-C5-H9	119.56	119.6414	119.6301	119.634	119.6228
C6-C5-H9	120.057	120.0853	120.0873	120.075	120.0772
C1-C6-C5	119.7332	119.6853	119.7707	119.6804	119.755
C1-C6-H10	119.7764	119.8309	119.7817	119.832	119.7955
C5-C6-H10	120.4902	120.4837	120.4475	120.4874	120.4493
C3-C11-N12	115.2722	114.8585	115.3178	114.6749	115.1494
C3-C11-O15	120.5307	120.5118	120.5817	120.5567	120.5548
N12-C11-O15	123.875	124.1315	123.7072	124.2923	123.8866
C11-N12-H13	115.8144	114.7257	116.3293	115.0125	116.2744
C11-N12-H14	119.3354	117.48	119.5092	117.7549	119.283
H13-N12-H14	116.7363	115.3259	117.0742	115.6925	117.0798
C2-N16-O17	117.7678	117.7686	117.8141	117.6843	117.7303
C2-N16-O18	117.0905	117.2884	117.3545	117.1495	117.2526
O17-N16-O18	125.1204	124.9316	124.8163	125.1525	125.0022

Dihedral Angle (°)					
C6-C1-C2-C3	–1.0091	–0.697	–1.1373	–0.7658	–1.1555
C6-C1-C2-N16	176.8431	177.4508	176.9525	177.1293	176.9215
H7-C1-C2-C3	179.5178	179.464	179.5239	179.4799	179.5107
H7-C1-C2-N16	–2.63	–2.3882	–2.3863	–2.6251	–2.4122
C2-C1-C6-C5	0.3858	0.3084	0.4541	0.2925	0.4699
C2-C1-C6-H10	–179.5073	–179.5693	–179.4038	–179.541	–179.3868
H7-C1-C6-C5	179.849	–179.8582	179.7749	–179.9619	179.7837
H7-C1-C6-H10	–0.0442	0.2641	–0.083	0.2046	–0.0731
C1-C2-C3-C4	0.936	0.3534	0.9839	0.5015	0.9811
C1-C2-C3-C11	–173.1128	–172.522	–171.9698	–172.2309	–172.0716
N16-C2-C3-C4	–176.8628	–177.7424	–177.0577	–177.3393	–177.0493
N16-C2-C3-C11	9.0885	9.3822	9.9886	9.9283	9.898
C1-C2- N16-O17	25.5148	16.9002	22.4557	18.5233	21.9369
C1-C2- N16-O18	–152.8936	–161.9383	–156.197	–160.1976	–156.729
C3-C2- N16-O17	–156.5814	–164.913	–159.4117	–163.534	–159.9411
C3-C2- N16-O18	25.0102	16.2485	21.9355	17.7451	21.393
C2-C3-C4-C5	–0.2555	0.3737	–0.1662	0.2273	–0.1396
C2-C3-C4-H8	–179.1085	–179.0928	–179.017	–179.13	–179.0241
C11-C3-C4-C5	174.1676	173.7685	173.2141	173.4402	173.3278
C11-C3-C4-H8	–4.6854	–5.6981	–5.6367	–5.917	–5.5566
C2-C3-C11-N12	–111.2264	–101.7148	–111.742	–105.3585	–111.4727
C2-C3-C11-O15	75.0428	86.0545	75.1947	82.226	75.5901
C4-C3-C11-N12	74.7422	85.4239	75.3431	81.9403	75.5146
C4-C3-C11-O15	–98.9886	–86.8097	–97.7202	–90.4753	–97.4226
C3-C4-C5-C6	–0.3305	–0.7522	–0.4788	–0.6837	–0.5075
C3-C4-C5-H9	–179.8526	179.6711	179.9806	179.7412	179.9487
H8-C4-C5-C6	178.5129	178.707	178.3505	178.6648	178.3639
H8-C4-C5-H9	–1.0092	–0.8697	–1.1811	–0.9102	–1.1799
C4-C5-C6-C1	0.2655	0.3992	0.3329	0.415	0.3397
C4-C5-C6-H10	–179.8422	–179.7239	–179.8101	–179.7526	–179.8045
H9-C5-C6-C1	179.7852	179.9739	179.8713	179.9881	179.8814
H9-C5-C6-H10	–0.3225	–0.1492	–0.2717	–0.1794	–0.2628
C3-C11-N12-H13	173.1876	171.3074	174.0636	171.4957	173.7856
C3-C11-N12-H14	25.5031	30.9223	24.3394	29.67	24.5916
O15-C11-N12-H13	–13.3175	–16.781	–13.1163	–16.4116	–13.5424
O15-C11-N12-H14	–161.002	–157.1661	–162.8405	–158.2373	–162.7364

Table 2: Observed and calculated vibrational frequencies of o-nitrobenzamide using HF and DFT (B3LYP & B3PW91) at the 6-31+& cc-pVDZ, aug cc-pVDZ level

Sl No.	**Observed Frequency(cm^{-1})**		**Methods**					**Vibrational Assignments**
			HF	**B3LYP**		**B3PW91**		
	FT-IR	**FT Raman**	**6-31 +G (d, p)**	**cc-pVDZ**	**aug-cc-pVDZ**	**cc-pVDZ**	**aug-cc-**	

							pVDZ	
1	3390vs	-	3483	3463	3504	3465	3502	υ_{N-H} (100%)
2	3390 vs	-	3364	3342	3378	3340	3373	υ_{N-H} (100%)
3	3180 s	-	3009	3060	3067	3044	3052	υ_{C-H} (95%)
4		3100 vw	2983	3035	3044	3023	3033	υ_{C-H} (97%)
5	2900 vw	-	2975	3026	3035	3014	3024	υ_{C-H} (97%)
6	2900 vw	-	2962	3014	3024	3002	3012	υ_{C-H} (100%)
7	1680 vs	-	1730	1705	1668	1709	1677	$\upsilon_{C=O}$ (84%)
8	1600 s	-	1626	1582	1571	1594	1581	$\upsilon_{N=O}$ (31%) + $\upsilon_{C=C}$ (36%)
9	1590 w	-	1578	1545	1537	1557	1547	$\upsilon_{N=O}$ (35%) + $\upsilon_{C=C}$ (33%)
10	1580 w	-	1672	1646	1647	1652	1646	$\upsilon_{N=O}$ (12%) + υ_{C-C} (43%)
11	-	1570 vw	1654	1628	1629	1615	1632	δ_{NH2} (74%)
12	1520 vs		1556	1532	1531	1527	1525	υ_{C-C} (14%) + δ_{HCC} (48%)
13	1470 m	-	1538	1490	1485	1483	1478	υ_{C-C} (13%) + δ_{HCC} (44%)
14	1430 w	-	1501	1423	1419	1443	1438	$\upsilon_{N=O}$ (77%) + δ_{ONO} (10%)
15	1400 m	1400 vw	1396	1391	1391	1403	1397	υ_{N-C} (30%) + $\upsilon_{C=C}$ (18%) + δ_{HNC} (13%) + δ_{NCO} (12%)
16	1400 m	1400 vw	1322	1388	1383	1393	1393	υ_{C-C} (78%)
17	1320 w	-	1255	1298	1303	1287	1291	δ_{HCC} (58%)
18	1270 w	1270 vw	1194	1196	1202	1191	1194	δ_{HCC} (67%)
19	1230 vw	-	1178	1271	1275	1280	1282	$\upsilon_{C=C}$ (17%) + υ_{N-C} (10%) + δ_{HCC} (29%)

20	1230 vw	-	1223	1257	1261	1261	1264	$\upsilon_{C=C}$ (15%) + δ_{HNC} (12%) + δ_{HCC} (24%)
21	1230 vw	-	1215	1216	1211	1218	1211	$\upsilon_{O=C}$ (12%) + $\upsilon_{N=C}$ (27%) + δ_{HNC} (42%)
22	1180 vw	-	1180	1184	1184	1156	1187	υ_{N-C} (12%) + δ_{CCC} (45%)
23	1130 m	-	1133	1157	1160	1163	1164	$\upsilon_{C=C}$ (71%) + δ_{HCC} (12%)
24	1130 m	-	1132	1109	1107	1108	1098	τ_{HCCN} (14%) + τ_{HCCC} (66%)
25	1090 vw	-	1100	1074	1070	1073	1067	τ_{HCCN} (40%) + τ_{HCCC} (42%)
26	1000 vw	1000 vw	1003	983	979	982	977	τ_{HCCN} (27%) + τ_{HCCC} (50%)
27	970 vw	970 vw	963	952	949	962	957	υ_{N-C} (10%) + γ_{CCC} (14%) + γ_{OCN} (47%)
28	890 vw	890 vw	899	875	879	878	882	τ_{HCCC} (54%) + γ_{OCON} (30%)
29	860 m	860 vw	859	844	849	844	849	γ_{OCON} (10%) + γ_{HCC} (50%)
30	850 vw	850 vw	838	833	835	833	834	δ_{CCC} (22%) + γ_{OCNC} (33%)
31	830 vw	-	823	828	824	829	825	γ_{OCNC} (27%) + γ_{NH2}
32	790 m	790 vw	785	778	780	780	781	τ_{HCCC} (11%) + τ_{CCCC} (25%) + γ_{OCON} (36%)
33	730 w	730 vw	728	741	739	741	740	υ_{N-C} (11%) + γ_{CCC} (29%) + γ_{ONO} (18%)
34	665 w	-	661	670	668	666	665	γ_{NCO} (40%) + γ_{CCC} (11%)
35	620 vw	-	617	631	626	629	625	τ_{HNCC} (38%)
36	600 vw	-	611	620	620	618.6	619	γ_{CCN} (21%) + τ_{HNCC} (14%) + τ_{CCCC} (13%)
37	570 vw	570 vw	567	1569	1368	1530	1368	γ_{CNO} (25%) + τ_{HNCC} (30%)

38	-	470 vw	467	1327	1128	1288	1123	τ_{HNCC} (76%)
39	-	440 vw	455	1265	1094	1224	1097	τ_{CCCC} (33%) + γ_{NCCC} (23%)
40	-	430 vw	1243	1218	1078	1193	1081	υ_{N-C} (30%) + γ_{CCC} (13%)
41	-	390 vw	1071	1038	930	1008	923	γ_{CCN} (20%) + τ_{CCCC} (52%)
42	-	360 vw	971	943	851	924	847	$\upsilon_{C=C}$ (15%) + γ_{CNO} (11%) + γ_{CCC} (17%) + γ_{CCN} (13%)
43	-	360 vw	788	775	685	752	681	γ_{CNO} (14%) + γ_{CCN} (46%)
44	-	360 vw	516	504	440	486	439	γ_{CCC} (12%) + γ_{NCCC} (24%) + γ_{CCCC} (22%)
45	-	360 vw	469	468	406	446	399	γ_{CCC} (44%) + γ_{CCN} (13%)
46	-	360 vw	333	309	276	299	276	τ_{CCCC} (41%) + γ_{CCCC} (32%)
47	-	360 vw	255	194	208	207	213	τ_{CCNO} (63%) + τ_{CCCN} (21%)
48	-	360 vw	103	73	84.37	74.91	84	τ_{CCNO} (21%) + τ_{CCCN} (65%)

The ^{1}H and ^{13}C NMR isotropic shielding are calculated using the GIAO method[Yanagimoto H., *et al.*, (2001)] and the optimized parameters obtained from the B3LYP/cc-pVDZ functional. ^{13}C isotropic magnetic shielding (IMS) of any X carbon atoms is made according to the ^{13}C IMS value of TMS, $CS_X = IMS_{TMS}\text{-}IMS_x$. The ^{1}H and ^{13}C isotropic chemical shifts of TMS (Tetramethylsilane) in gas, DMSO, methanol and ethanol are calculated usingIEFPCM methods with the B3LYP functional at the cc-pVDZ level. The absolute chemical shift is found between the isotropic peaks and the peaks of TMS [Gan J. H., *et al.*, (2004)].

4. Results and discussion

4.1.Molecular geometry

From the optimized output file of Gaussian, it is observed that the molecular structure of o-nitrobenzamide belongs to C_1 point group symmetry. The optimized structure of the molecule is obtained from the Gaussian 09 and Gauss view program[Kuo C. H., and Huang M. H., (2008)] and is shown in Fig. 1. The present molecule contains one nitro group and one amide group, which are loaded in the left moiety. The hexagonal structure of the benzene is deformed at the point of substitution due to the addition of the heavy mass. It is also evident that the bond length (C1—C2 & C2 —C3) at the point of substitution is 0.0054 Å, which is longer than the rest in the ring. Consequently, the property of the same also changed with respect to the ligand (nitro and amide groups). The bond angle of C1–C2–C3 is 2.0151º elevated than C4–C5–C6 in the ring, which also confirms the deformation of the hexagonal shield. Although both C=O and NH_2, the bond length values between C2–C3 and C3–C11 differed by 0.121 Å. The entire C–H bonds in the chain and the amide groups have almost equal inter-nuclear distance.

4.2. Vibrational assignments

In order to obtain the spectroscopic significance of o-nitrobenzamide, the computational calculations are performed using frequency analysis. The molecule has C_1 point group symmetry, consists of 18 atoms, so it has 48 normal vibrational modes. On the basis of C_1symmetry, the 48 fundamental vibrations of the molecule can be distributed as 36 in-plane vibrations of A′ species and 12 out-of-plane vibrations of A″ species, i.e., Γ_{vib} = 36 A′ + 12 A″. In the C_1 group, the symmetry of the molecule is a non-planar structure and has 48 vibrational modes that span in the irreducible representations.

The vibrational frequencies (unscaled and scaled) calculated at HF, B3LYP and B3PW91methods with 6-311+G(d,p), cc-pVDZ and aug cc-pVDZ basic sets and observed FT-IR and FT-Raman frequencies for various modes of vibrations have been presented in Tables 2 and 3. Frequencies calculated at the HF and B3LYP/B3PW91 method are found to the higher compared to experimental vibrations. Inclusion of electron correlation in the density functional theory to a certain extent makes the frequency values smaller in comparison with the HF frequency data.

The calculated frequencies are scaled down to give up the rational with the observed frequencies. The scaling

factors are 0.8889, 0.939, 0.9999 and 0.9909 for HF/6-31+G (d,p). For the B3LYP/cc-pVDZ/aug-cc-pVDZ basis set, the scaling factors are 0.9544, 1.0174, 1.0919 and 1.0881/0.9578, 1.0207, 1.0976 and 1.0929. For the B3PW91/ cc-pVDZ/aug-cc-pVDZ basis set, the scaling factors are 0.9466, 1.0105, 1.0939 and 1.0871/0.9511, 1.0125, 1.0968 and 1.0921.

4.2.1. N−H, N=O vibrations

In heterocyclic molecules, the N−H stretching vibrations have been measured in region 3500–3000 cm^{-1}[Bijani S., *et al.*, (2007)]. As seen in Table 2, the two N−H stretching modes are calculated at 3494 and 3372 cm^{-1} in B3LYP. A very strong IR N−H stretching vibration is observed at 3390 cm^{-1} in the experimental spectrum. Ten et al. have observed these modes at 3479 and 3432 cm^{-1}, respectively, for isolated thymine [Xu Y., *et al.*, (2007)]. In 2-amino-4-methylbenzothiazole, V. Arjunan et al., [Xu H., *et al.*, (2006)] have observed the vibrational frequencies at 3417 and 3287 cm^{-1}. Cirak and Koc have calculated the N–H stretching modes at 3189 and 3155 cm^{-1} for dimerictrifluorothymine[Guan L., *et al.*, (2010)]. However, no Raman band is observed for the N−H stretching modes in the experimental spectra.For primary amino group the in-plane $–NH_2$ deformation vibration occur in the short range 1650–1580 cm^{-1} region of the spectrum. Therefore the very weak band observed in IR at 1570 cm^{-1} is assigned to the deformation mode of the amino group. The most characteristic bands in the spectra of nitro compounds are due to NO_2 stretching vibrations, which are the most useful group wavenumbers, not only because of their spectral position but also for their strong intensity[Poizot P., *et al.*, (2000)]. The N=O stretching vibrations have been measured in region 1515-1560 cm^{-1}. A weak IR N=O stretching vibration is observed at 1430 cm^{-1}. However, no Raman band is observed for the N=O stretching modes. Hence these vibrations show good agreement with the literature values.

4.2.2. C–H Vibrations

The C–H stretching vibrations are normally observed in the region 3100 – 3000 cm^{-1} for the aromatic benzene structure,[Jiao S., *et al.*, (2006); Chen A., *et al.*, (2008)] which shows their uniqueness of the skeletal vibrations. The bands appeared at 3100, 3090, 3080, and 3050 cm^{-1} in o-nitrobenzamide are assigned to C–H ring stretching vibrations. The FT-IR bands at 1520 and 1470 cm^{-1} are assigned to C–H in-plane bending vibrations and FT-IR bands at 860 cm^{-1} are assigned to C–H out-of-plane bending vibration. V. Karunakaran*et al.*,

[AkhavanO., *et al.*, (2009)] in the molecule 4-chloro-3-nitrobenzaldehyde have observed the bands at 3053, 3034 cm^{-1} in FT-IR and at 3079, 3052 cm^{-1} in FT-Raman spectra. The FT-IR bands at 1467, 1422 cm^{-1} and the FT-Raman bands at 1423 and 1218 cm^{-1} were assigned to C–H in-plane bending vibration of CNB. The C–H out-of-plane bending vibrations of the CNB were well identified at 989, 822 and 722 cm^{-1} in the FT-IR and 828 cm^{-1} in the FT-Raman spectra V. Arjunan*et al.*, [Pang H., *et al.*, (2009)] In 4-acetyl benzonitrile, were observed the C–H stretching peaks in IR at 3075 and 3030 cm^{-1} and in Raman spectrum at 3090, 3074 and 3025 cm^{-1}. The frequencies calculated for the present compound using B3LYP/cc-pVDZ and B3LYP/aug cc-pVDZ methods for C–H in-plane bending vibrations showed excellent agreement with the recorded spectrum as well as literature data.

4.2.3. C–C vibrations

V. Arjunan*et al.*, [McShane C. M., and Choi K. S., (2009)] In 4-acetyl benzonitrile, have observed the C–C stretching vibrations at 1593, 1556, 1485, 1415, and 1259 cm^{-1} in IR spectrum and 1603, 1482, 1430, 1408 and 1270 cm^{-1} in Raman spectrum. The IR bands observed at 1593 and 1285 cm^{-1} were strong while the Raman band 1603 cm^{-1} was very strong. In addition, C–C–C in–plane bending vibrations have been attributed to 1002 and 844 cm^{-1} in IR spectrum and 794 cm^{-1} in Raman spectrum. The C–C–C out of plane vibrations have observed at 337, 227 and 108 cm^{-1} in Raman spectrum. V. Karunakaran*et al.*, [Altman R. A., *et al.*, (2007)] in the molecule 4-chloro-3-nitrobenzaldehyde have observed the C–C stretching vibrations at 1589, 1356, 1200 and 1056 cm^{-1} in FT-IR spectrum and at 1626, 1372, 1160 and 1058 cm^{-1} in Raman spectrum.

The bands due to the C–C stretching vibrations are called skeletal vibrations normally observed in the region 1430–1650 cm^{-1} for the aromatic ring compounds[Ng C. H. B., and Fan W. Y., (2006);Hara M., *et al.*, (1998)]. Socrates[Deng J., *et al.*, (1996)] mentioned that the presence of a conjugate substituent such as C=C causes stretching of peaks around the region of 1625–1575 cm^{-1}. As predicted in the earlier references, in this title compound, the prominent peaks are found with strong and medium intensity at 1600 and 1590 cm^{-1} due to C=C stretching vibrations. The C–C stretching vibrations are appeared at 1580, 1520, 1470 and 1400 cm^{-1}. The CC out-of-plane bending vibrations are appeared at 1130, 1090, 1000 and 970 cm^{-1}.

4.2.4. C−N vibrations

The C−N vibration of the compound identification is a very difficult task, since the mixing of several bands is possible in the region. Silverstein [Yuhas B. D., and Yang P., (2009)] assigned C−N stretching absorption in the region 1382–1266 cm^{-1} for aromatic amines. In benzamide the band observed at 1368 cm^{-1} is assigned due to C−N stretching [Petra E. de Jongh,*et al.*, (1999)]. However with the help of force field calculations, the C−N vibrations are identified and assigned in this study. A. Prabakaran et al.[31] in 7-(1,3-dioxolan-2-ylmethyl)-1,3-dimethylpurine-2,6-dione (7DDMP26D) have observed C–N, C=N stretching vibrations at 1478.19 and 1280.19 cm^{-1}in FT-IR spectrum and at 1480.00 and 1280.53 cm^{-1}in FT-Raman spectrum respectively. In our present work, C−N stretching vibrations are observed at 1400 and 1180 cm^{-1} in FT-IR spectrum. This band has been calculated at 1403 cm^{-1} by DFT method and at 1180 cm^{-1} by HF method in very good agreement with experimental values.

4.2.5. C=O vibrations

The C=O stretching frequency appears strongly in the IR spectrum in the range 1600–1850 cm^{-1} because of its large change in dipole moment. The carbonyl group vibrations give rise to characteristics bands in vibration spectra and its characteristic frequency used to study a wide range of compounds. The intensity of these bands can increase owing to conjugation or formation of hydrogen bonds [Lisiecki I., and Pileni M. P., (1993)]. Carthigayan*et al.*, [Kooti M., and Matouri L., (2010)] have observed the bands at 1822 and 1842 cm^{-1} in the infrared spectrum corresponds to C=O stretching in 4,5-Bis(bromomethyl)-1,3-dioxol-2-one (45BMDO). The corresponding frequency of 4-Bromomethyl-5-methyl-1,3-dioxol-2-one (4BMDO) was observed at 1820 cm^{-1}. A very strong IR absorption band at 1680 cm^{-1} is readily assigned to the carbonyl vibration in the o-nitrobenzamide; the corresponding DFT computed mode at 1720 cm^{-1} at B3LYP/cc-pVDZ, level is good agreement with the observed one.

4.3. NMR assessment

NMR spectroscopy is currently used for the structural elucidation of complex molecules. The combined use of experimental and computational tools offers a powerful gadget to interpret and predict the structure of bulky molecules. The optimized structure of o-nitrobenzamide is used to obtain the NMR spectra supported by the GIAO method with B3LYP functional at the cc-pVDZ basic set, and the chemical shifts of the compound are reported in ppm relative to

TMS for ^{1}H and ^{13}C NMR spectra, which are presented in Table 3. The corresponding spectra are shown in Fig. 4.

^{13}C NMR chemical shifts for similar organic molecules usually are >100 ppm. The accuracy ensures reliable interpretation of spectroscopic parameters. In the case of o-nitrobenzamide, the chemical shifts of C1, C2, C3, C4, C5, C6, and C11 are 132.429, 144.929, 122.479, 120.791, 118.984, 122.882 and 179.985 ppm respectively. The shift is higher in C2 and C11 than the others.

All the carbon atoms in the molecule are found to have higher chemical shifts it is because of presence of highly negative atoms attached to the carbons. Among this C11 atom has higher chemical shift compared to all other atoms. It is due to attachment of electrons withdrawal amide carbonyl functional group.

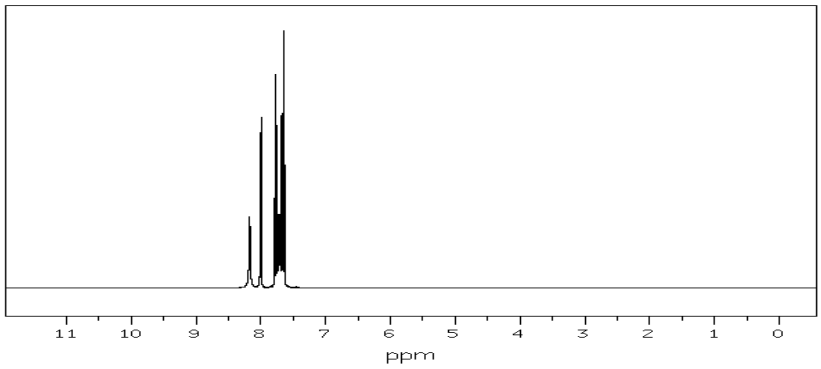

Figure 4: 1H NMR Spectrum of o-Nitrobenzamide

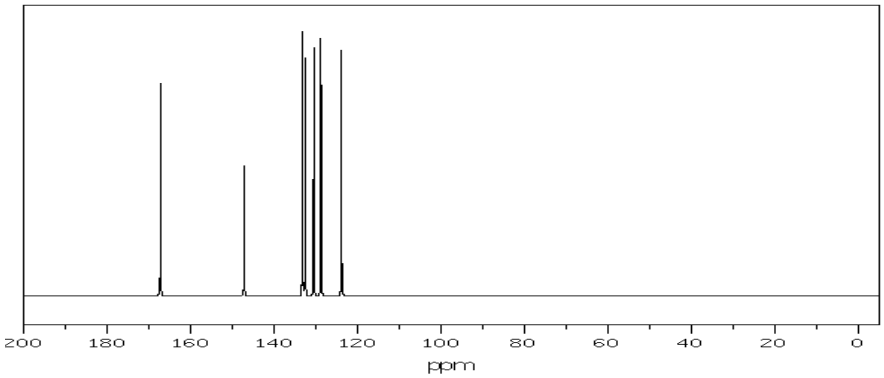

Figure 5: 13C NMR Spectrum of o-Nitrobenzamide

Table 3: Experimental and Calculated 1H and 13C NMR chemical shifts (ppm) of o-Nitrobenzamide

Atom position	Experimental Value (ppm)	Gas	Solvent		
			Methanol	Ethanol	DMSO
		B3LYP/cc-pVDZ GIAO (ppm)	B3LYP/cc-pVDZ GIAO (ppm)	B3LYP/cc-pVDZ GIAO (ppm)	B3LYP/cc-pVDZ GIAO (ppm)
C1	133	132.429	133.586	133.564	133.608
C2	147	144.929	144.798	144.797	144.8
C3	131	122.479	122.946	122.94	122.952
C4	128	120.791	122.979	122.937	123.021
C5	123	118.984	122.424	122.366	122.481
C6	132	122.882	125.152	125.114	125.188
C11	168	179.985	182.813	182.769	182.855
7H	-	6.7288	6.7987	6.7978	6.7995
8H	8.2	8.5839	8.7702	8.7671	8.7733
9H	7.6	7.554	7.8743	7.8691	7.8794
10H	7.8	7.637	7.9422	7.9374	7.9468
13H	-	2.8879	3.1966	3.1932	3.1999
14H	-	2.1573	2.6503	2.6419	2.6586

5. Conclusion

In the geometrical study, it is observed by the calculation of the bond length and bond angle, the hexagonal structure of the compound is deformed. In the vibrational study though most of the vibrations are in line with the literature some the mode corbonylgroups are shifted to the end position of the range. The NMR reveals that the C11 atom which is attached to the carbonyl and amine group has more shift compared all other atoms in the compound, it means that atom is more deshielded by its electrons.

References

Jiang P., BertoneJ. F., and Colvin V.L., (2001),A lost-wax approach to monodisperse colloids and their crystals, Science, 291:453-457.

Zhang H., and Cui Z.,(2008),Solution-phase synthesis of smaller cuprous oxidenanocubes, Mater. Res. Bull., 43:1583-1589.

Kuo C. H., Chen C. H., and Huang M.H., (2007),Seed-mediated synthesis of monodispersed Cu_2O nanocubes with five different size ranges from 40 to 420 nm, Adv. Funct. Mater., 17: 3773-3780.

Carnes C.L., Stipp J., and Klabunde K. J.,(2002), Synthesis, characterization, and adsorption studies of nanocrystalline copper oxide and nickel oxide, Langmuir, 18:1352-1359.

Wang H. W., Xu J. Z., Zhu J. J. and Chen H. Y.,(2002),Preparation of CuO nanoparticles by microwave irradiation, J. Cryst. Growth, 244: 88-94.

Yang Y., Chen H., Zhao B. and Bao X.,(2004),Size control of ZnO nanoparticles via thermal decomposition of zinc acetate coated on organic additives, J. Cryst. Growth, 263:447-453.

Deki S., Akamatsu K., Yano T., Mizuhata M. and Kajinami A., (1998),Preparation and characterization of copper (I) oxide nanoparticles dispersed in a polymer matrix
J. Mater. Chem., 8: 1865-1868.

Wang W., Wang G., Wang X., Zhan Y., Liu Y. and Zhang C., (2002),Synthesis and characterization of Cu_2O nanowires by a novel reduction route, Adv. Mater., 14: 67-69.

Yanagimoto H., Akamatsu K., Gotoh K., and Deki S., (2001),Synthesis and characterization of Cu_2O nanoparticles dispersed in NH_2-terminated poly (ethylene oxide), J. Mater. Chem., 11: 2387-2389.

Gan J. H., Yu G. Q., Tay B. K., Tan C. M., Zhao Z. W., and Fu Y. Q., (2004),Preparation and characterization of copper oxide thin films deposited by filtered cathodic vacuum arc, J. Phys D: Appl Phys.,37: 81-85.

Swarnkar R. K., Singh S. C., and Gopal R., (2009), AIP Conf. Proc., 1147: 205-207.

Huang L., Peng F., Yu H., and Wang H., (2009),Preparation of cuprous oxides with different sizes and their behaviors of adsorption, visible-light driven photocatalysis and photocorrosion, Solid State Sci., 11:129-138.

Kuo C. H., and Huang M. H., (2008), Fabrication of truncated rhombic dodecahedral Cu_2O nanocages and nanoframes by particle aggregation and acidic etching, J. Am. Chem. Soc., 130: 12815-12820.

Bijani S., Gabas M., Maryinez L., Ramos Barrado J. R., Morales J., andSanchez L., (2007),Nanostructured Cu_2O thin film electrodes prepared by electrodeposition for rechargeable lithium batteries, Thin Solid Films, 515: 5505-5511.

Xu Y., Chen D., Jiao X., and Xue K.,(2007),Nanosized Cu_2O/PEG400 composite hollow spheres with mesoporous shells, J. Phys. Chem. C, 111:16284-16289.

Xu H., Wang W., and Zhu W.,(2006), Shape evolution and size-controllable synthesis of Cu_2O octahedra and their morphology-dependent photocatalytic properties, J. Phys. Chem. B, 110: 13829-13834.

Guan L., Pang H., Wang J., Lu Q., Yin J., and Gao F.,(2010),Fabrication of novel comb-like Cu_2O nanorod-based structures through an interface etching method and their application as ethanol sensors, Chem. Commun., 46: 7022-7024.

Poizot P., Laruelle S., Grugeon S., Dupont L., and Tarascon J. M.,(2000),Nano-sized transition-metal oxides as negative-electrode materials for lithium-ion batteries, Nature, 407:496-499.

Jiao S., Xu L., Jiang K., and Xu D.,(2006), Well-Defined Non-spherical Copper SulfideMesocages with Single-Crystalline Shells by Shape-Controlled Cu_2O Crystal Templating, Adv. Mater., 18: 1174-1177.

Chen A., Haddad S., Wu Y. C., Fang T. N., Kaza S., and Lan Z., (2008), Erasing characteristics of Cu_2O metal-insulator-metal resistive switching memory, Appl. Phys. Lett., 92:013503.

Akhavan O., Tohidi H., and Moshfegh A. Z.,(2009), Synthesis and electrochromic study of sol–gel cuprous oxide nanoparticles accumulated on silica thin film, Thin Solid Films, 517: 6700-6706.

Pang H., Gao F., and Lu Q., (2009),Morphology effect on antibacterial activity of cuprous oxide, Chem. Commun., 9: 1076-1078.

Deng J., Sun Q., Zhang Y., Chen S., and Wu D., (1996), A novel process for preparation of a $Cu/ZnO/Al_2O_3$ ultrafine catalyst for methanol synthesis from $CO_2 + H_2$: comparison of various preparation methods, Appl. Catal. A, 139:75-85.

Ng C. H. B., and Fan W. Y.,(2006), Shape evolution of Cu_2O nanostructures via kinetic and

thermodynamic controlled growth,J. Phys. Chem. B, 110: 20801-20807.

Hara M., Kondo T., Komoda M., Ikeda S., Shinohara K., and Tanaka A., (1998),Cu_2O as a photocatalyst for overall water splitting under visible light irradiation, Chem. Commun., 3:357-358.

McShane C. M., and Choi K. S., (2009),Photocurrent enhancement of n-type Cu_2O electrodes achieved by controlling dendritic branching growth, J. Am. Chem. Soc.,131: 2561-2569.

Altman R. A., Koval E. D., and Buchwald S.L., (2007),Copper-catalyzed N-arylation of imidazoles and benzimidazoles, J. Org. Chem.,72: 6190-6199.

Tan Y., Xue X., Peng Q., Zhao H., Wang T., and Li Y., (2007),Controllable fabrication and electrical performance of single crystalline Cu2O nanowires with high aspect ratios, Nano. Lett., 7: 3723-3728.

Yuhas B. D., and Yang P., (2009),Nanowire-based all-oxide solar cells, J Am. Chem. Soc., 131: 3756-3761.

Petra E. de Jongh, Vanmaekelbergh D., and Kelly J. J., (1999), Cu_2O: a catalysis for the photochemical decomposition of water? Chem. Commun., 99: 1069-1070.

Yuhas B. D., and Yang P., (2009),Nanowire-based all-oxide solar cells, J Am. Chem. Soc., 131: 3756-3761.

Lisiecki I., and Pileni M. P., (1993), Synthesis of copper metallic clusters using reverse micelles as microreactors, J. Am. Chem. Soc., 115(1993): 3887-3896.

Kooti M., and Matouri L., (2010),Fabrication of Nanosized Cuprous Oxide using Fehling's Solution, ScientiaIranica Transaction F: Nanotechnology, 17: 73-77.